Asian Journal of Chemistry; Vol. 33, No. 7 (2021), 1656-1662

ASIAN JOURNAL OF CHEMISTRY

https://doi.org/10.14233/ajchem.2021.23319

Carbon Nanotube and Ethylene-Vinyl Acetate Based Soft Nanocomposite Film: Preparation and Characterization

N. GOPAL, A. SAXENA, B. KUMAR and R. SAHNEY*

Amity Institute of Biotechnology, Amity University Uttar Pradesh, Noida-201303, India

*Corresponding author: Fax: +91 120 2431878; Tel: +91 120 2432780-85; E-mail: rsahney@amity.edu; rachanasahney@gmail.com

Received: 18 May 2021; *Accepted*: 31 May 2021; *Published online*: 26 June 2021; AJC-20410

Soft and conductive interfaces are valuable in wearable electronics as they are capable for integration of diverse classes of electronic and sensor technologies directly with living body which can be used as health monitoring systems. In present work, we explore the development of multi-walled carbon nanotube-ethylene vinyl acetate nanocomposite (MWCNT-EVA) film and their properties. Oxidation of MWCNT is known to improve their dispersion properties and increase the electrical conductivity of MWCNT-polymer nanocomposites. Thus, pristine MWCNTs (*p*-MWCNTs) and functionalized MWCNTs (*f*-MWCNTs) were further used as conductive filler to construct *p*-MWCNT-EVA and *f*-MWCNT-EVA nanocomposite films. The films were characterized by Fourier-transform infrared spectroscopy, scanning electron microscopy, energy dispersive X-ray analysis and electrochemical technique. The results indicated that the chemical oxidation of *p*-MWCNT generates carboxylic function at the *p*-MWCNT surface important for sensor fabrication. The concentration of carboxylic functional group in *f*-MWCNT higher than in nanocomposites. The *f*-MWCNT-EVA nanocomposite film electrode surface show much higher conductivity than *p*-MWCNT-EVA nanocomposite film. Thus, the soft and flexible *f*-MWCNT-EVA nanocomposite films are effective for the development of electrochemical platform for biosensor fabrication in wearable applications.

Keywords: Pristine, Ethylene, Vinyl Acetate, Flexible nanocomposites, MWCNT-EVA nanocomposite films.

INTRODUCTION

Flexible electronics offers a wide variety of usages [1] in sensors for wearable, automobile and robotic applications where sensor flexibility is required for coverage of curved or dynamically moving surfaces. These systems require high-performance flexible electrodes, which are indispensable for all electronic devices and demand novel approaches in material design. Carbon nanotubes (CNTs) are promising material due to their conductivity [2,3] and their use as electrode [4-8]. With the breakthrough introduction by Iijima in 1991, CNTs have found their versatile applications reported in many areas due to their extraordinary electrical, mechanical and chemical properties, ultra-small size, large surface area and ability to conjugate variety of therapeutic molecules (drugs, proteins, antibodies, DNA, enzymes, *etc.*) [9]. CNTs show maximum current density of 10^7-10^9 A.m^2, tensile strength > 50× that of steel [10] and thermal conductivity greater than that of diamond [11], proving CNTs as the best material to be used as advanced filler materials in composites and for preparing conductive sensing platforms. Due to the compatibility of CNTs with biomolecules chemically and dimensionally, ability to facilitate the electron transfer between electrode surface and biomolecules, they are widely used in the construction of biosensors [12].

Achieving a uniform CNT dispersion has become a demanding issue for the preparation of CNT based films. Agglomerations of CNT and non-uniformity of composite had been reported in large number of literatures [13]. Making high performance flexible electrode requires sophisticated techniques and skilled engineering. Earlier approaches include direct CNT deposition on metal alloys [14], transfer of CNTs onto a conducting polymer [15], and growing CNTs on a carbon layer [16]. Although theoretically attractive, these approaches are somehow inconvenient because of the complex procedures and/or expensive experimental set-up [17]. Excellent properties of CNTs are being widely incorporated into polymers to produce composite materials where polymers offers high flexibility, low cost, light weight and easy fabrication [18,19]. Recently,

CNT-polymer composites films have attracted great attention of researchers as these composites has reported significant and multi-fold improved properties than its constituting materials [20,21] with reports on their applications in medical [22], electronics [23], supercapacitors [24] and environmental fields [25].

Non-reactive and inert surface of pristine CNTs limits its applications in composites because of lacking adhesion between CNTs and various matrix polymers. Intrinsic van der Waals attraction among tubes often leads to significant agglomeration, thus preventing efficient transfer of their superior properties to the matrix [26]. Functionalization of CNTs by acid treatment is the simple way to successfully oxidize the surface of multiwalled carbon nanotubes (MWCNTs) which leads to increased dispersibility of the CNTs in various organic solvents and polymers and also increase the strength of interface between CNT and the polymer matrix [27,28]. Improvements in electrical property of CNT-polymer composites due to functionalization of CNTs have clearly indicated that CNTs can provide continuous three-dimensional (3D) conducting paths within composite structure [29].

Tremendous work has been done in preparing composites based on CNTs and conducting polymers [30-32]. However, it should be noted that the complicated microstructures of these conducting polymers suffers from lack of reproducibility, controllability, stability and processibility for their applications in nano-devices [33]. Since last few years, indium tin oxide (ITO) films deposited on flexible organic substrates are being prepared in order to get thin, conducting and transparent films [34]. Since the ITO is brittle in nature and can form cracks while fabricating composite, some researchers were interested in applying the conducting polymer films to maintain electrical continuity if cracks are formed [35]. Additionally, the ITO surface is active when in contact with a corrosive or organic material, resulting in interface instability [36]. Therefore, there is a great need for alternatives to ITO which can overcome these limitations.

Ethylene-vinyl acetate (EVA) is low-cost, thermoplastic, recyclable, mainly applied for electrical cables, water proofing, corrosion protection and packaging applications with significant commercial importance, therefore, used as polymeric matrix for preparing CNT-polymer composite flexible films [37]. EVA shows a glass transition temperature around 30 ºC and is soluble in some aromatic solvents at high temperatures at ~90 ºC [38]. Interesting studies are being done in developing CNT-EVA composite films [39] and it is finding applications in many areas such as in biomedical [40], drug delivery [41] and other fields [42]. Since, EVA provides excellent adhesiveness on substrate with their low softening point and low melt viscosity and are easy to process at temperature below degradation [43], hence is an excellent material for fabricating low cost and flexible sensing platforms.

In present study, we have used the pristine MWCNTs (*p*-MWCNTs) and functionalized MWCNTs (*f*-MWCNTs) as filler material with ethylene-vinyl acetate (EVA) as matrix and studied the behaviour and benefits of integrating MWCNT with EVA matrix. The dispersion of *p*-MWCNT and *f*-MWCNT in organic matrix was determined by morphological and structural studies. Finally, the electrochemical response is evaluated by voltammetry. The characterization of the basic properties of these nanocomposites can help to understand and enhance their electrochemical response and improve their performance as biosensing electrode material.

EXPERIMENTAL

Pristine multiwalled carbon nanotubes (*p*-MWCNT) (specifications: 10-30 nm diameter and 0.2-2.00 μm length) were purchased from Chengdu Organic Chemistry Co. Ltd. Ethylene-vinyl acetate (EVA) films (0.2 mm) was bought from Swasan Chemicals Pvt. Ltd, Mumbai, India. Sulfuric acid, potassium ferricyanide, sodium hydroxide pellets, phosphate buffer and potassium chloride were bought from Fisher Scientific. Nitric acid, hydrochloric acid, sodium bicarbonate and ethanol was supplied from Merck, India. Double distilled water was used throughout the experiments for making solutions.

Functionalization of *p*-MWCNT and fabrication of *f*-MWCNT-EVA nanocomposite film electrode: Acid oxidation of MWCNTs was performed as given in reference [8]. In short, oxidation of MWCNTs was done by continuous stirring 50 mg of *p*-MWCNTs in the mixture of H_2SO_4 and HNO_3 [3:1 (v/v)] in a round bottom flask at 60 ºC for 6 h. The resulting functionalized MWCNTs (*f*-MWCNTs) were washed with double distilled water till the pH reached 7. The *f*-MWCNTs are then dried properly by keeping it in an oven at 120 ºC for 24 h. Further, 50 mg of *f*-MWCNTs was weighed and placed in a leak-proof glass bottle (15 mL) with spatula. In bottle, ethanol (1.0 mL) was added at an interval of 1 h with continuous sonication for 8-10 h while maintaining the temperature below 40 ºC. Uniformly dispersed *f*-MWCNT-ink so produced was then transferred manually to a clean glass slide covering area of 6 cm × 2 cm with the help of doctors blade method. The *f*-MWCNT film on glass slide was kept overnight at room temperature to evaporate ethanol and proper drying of the film. A piece of EVA film (6 cm × 2 cm) was overlaid on MWCNTs film over glass slide and heated on hot plate at 65 ºC to develop a *f*-MWCNT-EVA nanocomposite film by thermal transfer technique. Finally, *f*-MWCNT-EVA nanocomposite film was cut to 7.0 mm × 0.3 mm in size using sharp scissors and fixed onto printed circuit board (PCB) by using epoxy silver adhesive. A wire was attached to the piece of *f*-MWCNT-EVA nanocomposite films by soldering. Similarly, *p*-MWCNT-EVA nanocomposite film electrode was prepared by using *p*-MWCNT-ink instead of *f*-MWCNT-ink. These electrodes are used as working electrodes in all the electrochemical measurements.

Characterization

Measurement of surface functional group by potentiometric titration: Quantification of different oxygen functional groups present at *f*-MWCNT and *f*-MWCNT-EVA nanocomposite film surface was done by Boehm titration method [8]. Small amount of *f*-MWCNTs (0.2 mg) and pieces of *f*-MWCNT-EVA nanocomposite film containing same amount of *f*-MWCNT were placed in separate beakers containing 10.0 mL NaOH (0.04 N) solution in each. After stirring the mixture for 0.5 h, each beaker was kept overnight for further 18 h to reach the equilibrium state at room temperature. A pH meter (Hanna

HI5522-01) was used to titrate the resulting CNT and NaOH mixture by using 0.04 N HCl. A blank titration was performed with 10 mL NaOH (0.04 N) and HCl solution. Titration curves and first derivative plots were drawn to calculate amount of oxygen functional group produced by chemical oxidation method. Similarly, carboxylic group present at *f*-MWCNT and *f*-MWCNT-EVA nanocomposite film surface was measured by potentiometric titration as above using $NaHCO_3$ solution (0.04 N) in place of NaOH solution. All the experiments were executed at room temperature in triplicate. Amount of oxygen functional groups and carboxylic functional groups generated were calculated using titration curves.

FTIR spectral study: In order to understand different functionalities present on MWCNTs and MWCNT-EVA nanocomposite films, FT-IR spectra were measured by Bruker infrared spectrometer (Tensor 37) after taking small sections of MWCNT-EVA nanocomposite films placed on KBr discs. The analysis was conducted in transmission mode in spectral range from 4000 to 500 cm^{-1}.

Surface morphological study of MWCNT-EVA nanocomposite film: The morphologies of *f*-MWCNT-EVA nanocomposite film were studied and compared with *p*-MWCNT-EVA nanocomposite film, by performing scanning electron microscopy (SEM, Zeiss EVO 50). Ultra-thin sections of the samples were transferred at a 400-mesh copper grid, assembled onto the stage of the instrument and electron beam was focussed on it. Images were collected by microscope operating at accelerating voltage of 100 kU. The elemental study for determining composition of same nanocomposite film samples was done by SEM coupled with energy dispersive X-ray analysis (EDX) equipment.

Electrochemical measurements: Electrochemical characterization of fabricated electrodes was performed with Potentiostat Gamry Interface 1000 model no. ESA 410, USA using a conventional three electrode setup consisting of a working electrode (fabricated nanocomposite film electrode), Ag/AgCl reference electrode and a platinum wire as a counter electrode. All the measurements were conducted in 5.0 mL of solution containing 5 mM $K_3[Fe(CN)_6]$, 0.1 M KCl, 0.1 M sodium phosphate buffer at pH 7.4. Potential range of ± 1.0 V and scan rate of 50 mV/s was used.

RESULTS AND DISCUSSION

In recent years soft, flexible polymer nanocomposites containing MWCNT nanofillers have attracted enormous interest in interfacial communication and interactions between the nanofiller and the polymer matrix for sensing applications. Herein, a robust 3D superhydrophobic composite with multi-walled carbon nanotube/ethylene vinyl acetate (CNT/EVA) as its skeleton is proposed for development of conductive nanocomposite films. The *f*-MWCNT-EVA nanocomposite film was designed to fabricate a new sensing electrode by blending the electrical properties of carbon nanotubes to the nonconducting flexible polymer films. The schematic fabrication process of the flexible nanocomposite film using *f*-MWCNT and hydrophobic EVA is illustrated in Fig. 1. The overall steps includes: (a) MWCNT and solvent mixture, (b) distribution of MWCNT in ethanol to form a homogeneous CNT-ink, (c) MWCNT ink casting on a glass slide, (d) EVA film casting on the dried CNT-ink platform and simultaneous thermal transfer of *f*-MWCNT onto the EVA film surface by heating at 60 °C to form (e) flexible *f*-MWCNT-EVA nanocomposite film.

Measurement of surface functional group by potentiometric titration: Despite their numerous advantages, CNTs also suffer from a few drawbacks. Because of the nanometric dimensions, CNTs have a strong tendency to aggregate which restricts their applications and it can be improved by functionalization of MWCNTs [27]. Thus, simple acid oxidation of *p*-MWCNTs was performed as reported earlier [8] to create *f*-MWCNTs with modified surface properties, reduced degree of entanglements and improved solubility in polar solvents. The oxidation process produces multiple hydrophilic functional groups at MWCNT surface [44,45]. But carboxyl functions are most pertinent for biomolecule immobilization [46] by activation using carbodiimide [47]. Thus, Boehm titration [48] was applied to determine the effectiveness of the oxidation process. Sodium hydroxide base (NaOH; $pK_a = 15.7$) was chosen for acid base titration as it deprotonates all acidic oxygen functional groups (*i.e.* carboxyl, lactones, phenols) present at the surface of tubes and $NaHCO_3$ ($pK_a = 10.3$) was chosen for estimation of surface carboxylic group as it neutralizes carboxyl group in aqueous medium. Potentiometric titration curves are

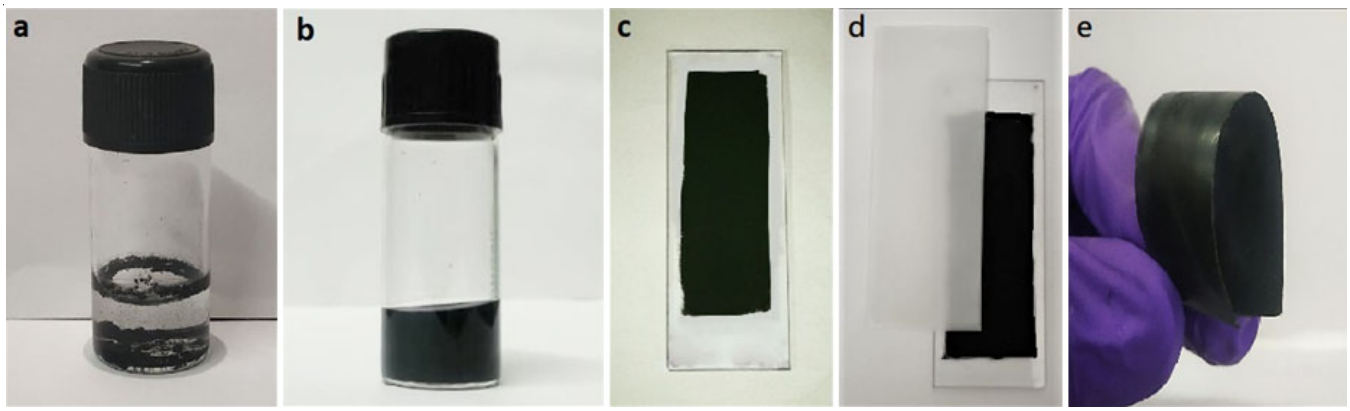

Fig. 1. Over-all steps involved in fabrication of MWCNT-EVA nanocomposite films: (a) MWCNTs added in solvent, (b) MWCNT-ink after dispersion, (c) MWCNT film on glass slide before casting EVA adhesive film, (d) EVA film over MWCNT ink on glass slide and (e) flexible MWCNT-EVA nanocomposite film

shown in Fig. 2(a&c) for *f*-MWCNT and the nanocomposite film (*f*-MWCNT-EVA) respectively and corresponding first derivative graphs are represented in Fig. 2(b&d). The strong acid-base titration shows equivalence point at pH 7.0. In present studies, strong base (NaOH and $NaHCO_3$) have been titrated with surface generated oxygen function group which are not strong acids. However, equivalence point was not clear from the potentiometric titration curves. Thus, equivalence point was determined by first derivative plot and concentration of acidic oxygen functions and carboxylic functional groups were calculated. The potentiometric quantification of surface carboxylic groups attained in *f*-MWCNT and *f*-MWCNT-EVA nanocomposite film are 1.2949 mmol/g of MWCNT and 1.1466 mmol/g, respectively.

Most of the polymer-MWCNT nanocomposite electrodes are fabricated by solution casting method. But here we have used thermoplastic EVA film (0.2 mm) and directly casted the film at the *f*-MWCNT layer on the glass slide which reduces solvent and plasticizer application in nanocomposite film making process. The maximum amount of CNT filler that can be homogeneously incorporated in a polymeric host matrix is limited. For electrochemical sensor applications, the electrical properties of the MWCNT-EVA nanocomposite are important. These can be controlled by the MWCNT content and its dispersion in the EVA. Thus, different MWCNT-EVA nanocomposites films were prepared with varying CNT content. The cyclic voltammetry was performed at a scan rate 50 mV/s between the potential ± 1.0 V. Nanocomposite electrodes with reproducible, large peak current (I_p), accompanied by the smallest difference in peak potential (ΔE_p) and no visible cracks at the electrode surface were chosen as working electrodes for sensor fabrication. Thus, in present experiments, a nanocomposite film containing 0.03455 g of *p*-MWCNT and 0.03515 g of *f*-MWCNT per gram of EVA film (3.45 %wt. and 3.51 %wt.), respectively were chosen as electrode material (*p*-MWCNT-EVA and *f*-MWCNT-EVA nanocomposite film electrode) for further studies, as it showed uniform dispersion of CNTs in EVA matrix with reproducible electrical properties.

FTIR spectra of MWCNT and MWCNT-EVA nanocomposite films: The FTIR spectrum of *p*-MWCNT is almost featureless as the characteristic of the sp^2 carbon present in CNTs and not shown here. However, the oxidation treatments lead to the appearance of new bands with comparatively high intensity (Fig. 3a) with peaks at 3294 cm^{-1} (O-H stretching vibration), at 2918 cm^{-1}, 2850 cm^{-1} (C-H stretching vibration in methyl/methylene), 1742 cm^{-1} (C=O stretching in carboxylic acid) and 1390 cm^{-1} (C-H stretching vibration). The MWCNTs were further used to develop nanocomposites by transferring the two different CNTs (*p*-MWCNT *&* *f*-MWCNT) to the EVA film surface by heating at 65 °C (Fig. 3b and 3c).

The *p*-MWCNT-EVA composite shows (Fig. 3b) peaks at 2918 cm^{-1} and 2850 cm^{-1} (C-H stretching vibration in methyl/

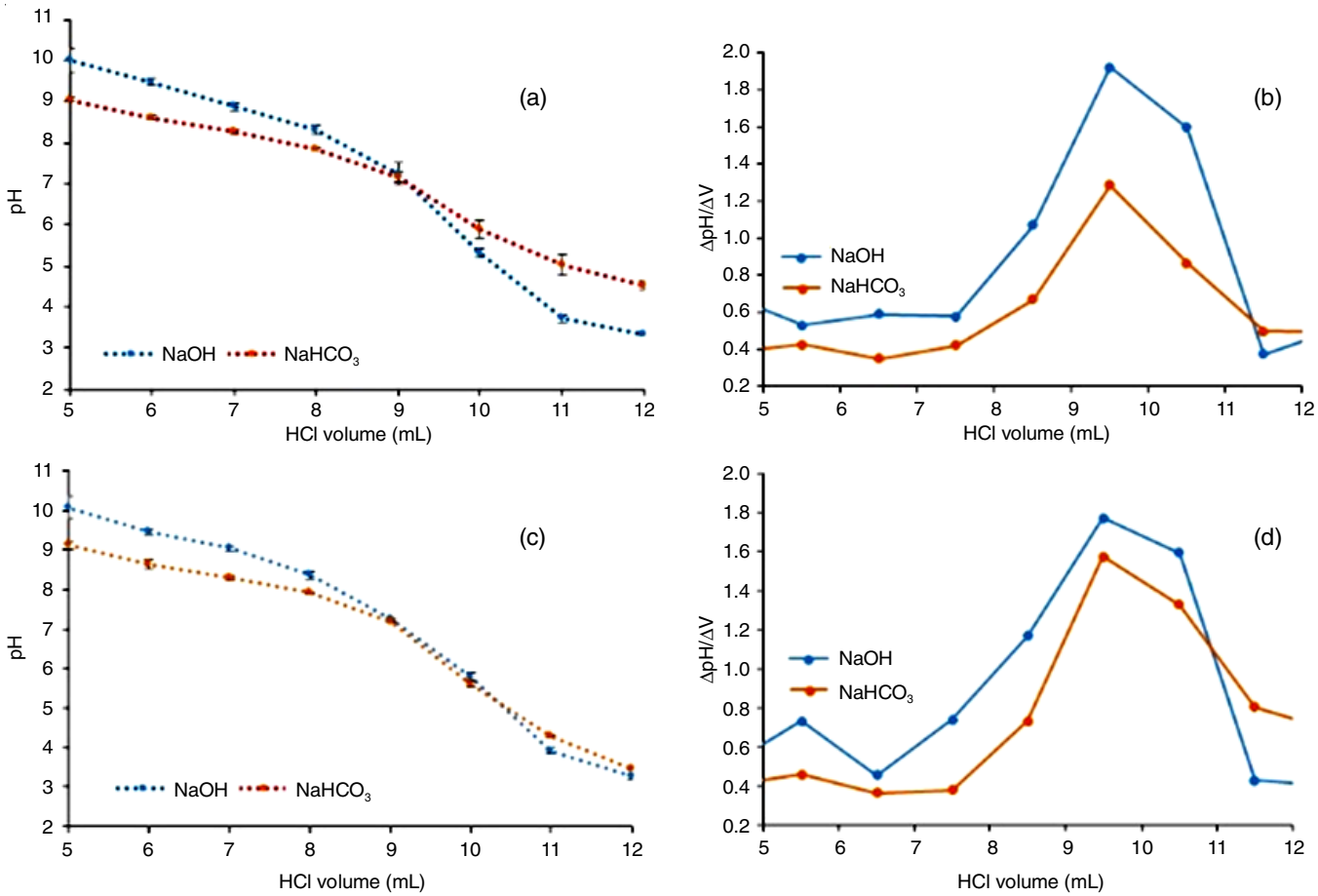

Fig. 2. Potentiometric titration curves and first derivative of the titration curves of *f*-MWCNT (a & b respectively) and *f*-MWCNT-EVA nanocomposite film (c & d respectively) in NaOH and $NaHCO_3$ against HCl as titrator solution

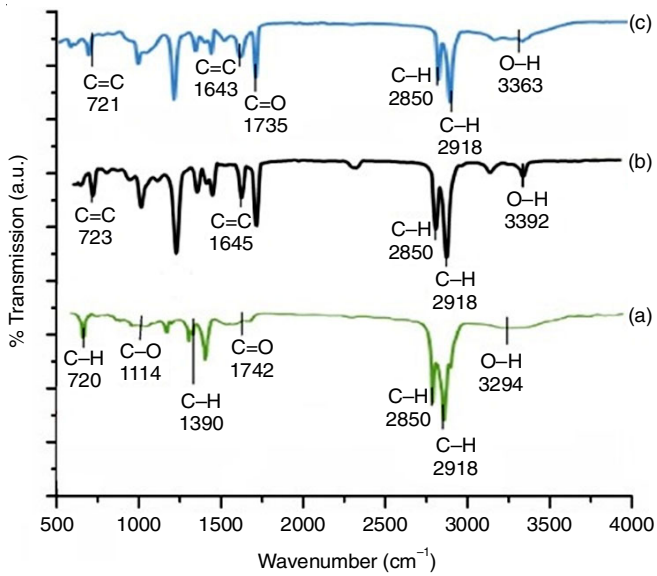

Fig. 3. FTIR spectra of (a) *f*-MWCNT, (b) *p*-MWCNT-EVA nanocomposite film, and (c) *f*-MWCNT-EVA nanocomposite film

methylene), 1645 cm^{-1} (C=C stretching vibration) and 723 cm^{-1} (C–H deformation) [49]. Hydrophobic interaction between polyethylene segments of EVA and *p*-MWCNT may occur [36] but IR spectrum of *p*-MWCNT-EVA nanocomposite film shows absorption bands characteristic of EVA polymer films. The low intensity peaks at 3188 and 3392 cm^{-1} (O-H stretching vibration) could be due to presence of moisture as impurities.

The *f*-MWCNT-EVA nanocomposite film shows absorption band (Fig. 3c) at 2918 cm^{-1}, 2850 cm^{-1} (C-H stretching vibration), 1735 cm^{-1} (C=O stretching vibration), 1643 cm^{-1} (C=C stretching vibration) and 721 cm^{-1} (C–H deformation) characteristic of EVA polymer films similar to Fig. 3b. A broad band at 3363 cm^{-1} (O-H stretching vibration) is characteristic of hydroxyl group present in *f*-MWCNT. These results confirmed that characteristics of *f*-MWCNT and EVA films incorporated in the nanocomposite.

Morphological studies of MWCNT-EVA nanocomposite films: MWCNT-EVA nanocomposite films were successfully fabricated by casting EVA film onto MWCNT films developed on glass slide with fixed dimensions and controlling the concentration of MWCNT deposition. The film casting procedure allowed the fabrication of thin films with a relatively flat surface without significant differences between the different formulations. After the fabrication step, SEM images were acquired to qualitatively investigate the dispersion of CNTs within the polymer film. The representative micrographs of the nanocomposites containing *p*-MWCNT (3.45 %) and *f*-MWCNT (3.51 %) as nanofillers are shown in Fig. 4a & 4b, respectively. MWCNTs distribution appears to be rather homogenous in the entire polymer matrix and no large agglomerates were observed (Fig. 4a-b). However, from the comparison of *p*-MWCNT-EVA and *f*-MWCNT-EVA nanocomposite film images, it is clear that *f*-MWCNTs are more evenly blended. The *p*-MWCNTs tend to bundle together because of the van der Waals interaction between the individual nanotubes. In contrast to pristine carbon nanotubes, *f*-MWCNTs have relatively low tube tube interactions. It is related to the hydrophilic groups that are located on the *f*-MWCNTs surfaces. Consequently, a very uniform dispersion of *f*-MWCNTs in the EVA matrix was obtained (Fig. 4b).

The elemental compositions of different nanocomposite films were studied by energy-dispersive X-ray analysis. EDX data shown in Table-1 reveals that the constituent elements present in two different nanocomposites are similar except few differences. The *p*-MWCNT-EVA nanocomposite film contains carbon (87.87 wt.%) while *f*-MWCNT-EVA nanocomposite film has a lower weight percent of carbon (81.32 wt.%) and

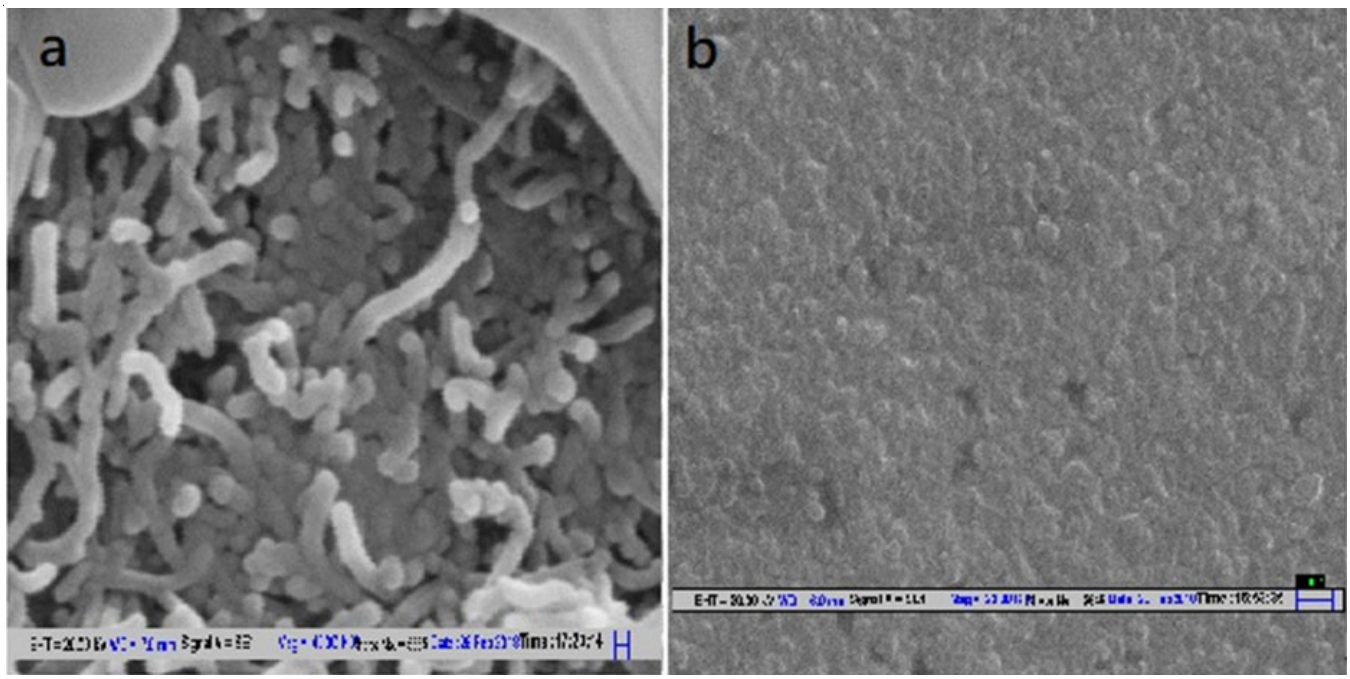

Fig. 4. SEM images of (a) *p*-MWCNT-EVA nanocomposite film and (b) *f*-MWCNT-EVA nanocomposite film

TABLE-1
EDX DATA SHOWING THE ELEMENTAL COMPOSITION OF *p*-MWCNT-EVA NANOCOMPOSITE FILM AND *f*-MWCNT-EVA NANOCOMPOSITE FILM

Element	Weight (%)	
	p-MWCNT-EVA nanocomposite film	*f*-MWCNT-EVA nanocomposite film
C	87.87	81.32
O	–	15.13
Ni	3.91	1.02
F	1.36	2.34
Cl	2.43	0.19
N	–	–
Na	–	–
S	1.47	–

higher weight percent of oxygen (15.13 wt.%), suggesting the oxidation of *p*-MWCNT surface and formation of oxygen based functionalities at the nanotube surface (-COOH, -OH) which are retained after nanocomposite film formation.

The presence of trace amounts of Ni, F, Cl and Na suggests that the metal and halogen impurities are introduced during CNT synthesis at manufacturer's level.

Electrochemical study

Voltammetric measurement of GCE, *p*-MWCNT-EVA nanocomposite film electrode and *f*-MWCNT-EVA nanocomposite film electrode: The stability of *p*-MWCNT-EVA and *f*-MWCNT-EVA nanocomposite films allowed us to use it as sheet type electrode and electrochemical activity of fabricated electrodes in PBS buffer was measured by cyclic voltammetry (CV) at different fabrication steps. In order to understand the electrochemical response of different nanocomposite films, CV was performed with standard redox species (potassium ferricyanide) sensitive towards the surface characteristics [50]. The results were compared with glassy carbon electrode (GCE) to establish their electrochemical performance. Cyclic voltammogram of GCE, *p*-MWCNT-EVA nanocomposite film electrode and *f*-MWCNT-EVA nanocomposite film electrode in sodium phosphate buffer containing 5 mM $K_3[Fe(CN)_6]$ and 0.1 M KCl at the scan rate of 50 mV/s has been shown in Fig. 5(a-c). Cyclic voltammogram of each electrode was characterized by a pair of well-defined redox peak with considerable differences in peak heights. The large difference in anodic (I_{pa}) and cathodic (I_{pc}) peak currents of nanocomposite films are attributed to large electroactive surface area of nanocomposite films that shows greatly enhanced faradaic response. A comparison of different nanocomposite films shows that the current response of *f*-MWCNT-EVA nanocomposite film electrode is higher than *p*-MWCNT-EVA nanocomposite film electrode which could be attributed to the presence of carboxylic group present at the MWCNT surface [51,52]. The current increment could be ascribed to acid treatment which creates more oxide defects on the side-walls, making *f*-MWCNT hydrophilic [49]. Thus, *f*-MWCNT embedded in the EVA matrix with partial hydrophilic characteristics shows better interaction with the aqueous interface than *p*-MWCNT. These results confirmed that MWCNTs were efficiently incorporated with the polymer matrix on nanocomposite surface, providing the essential conduction paths to promote the electron transfer.

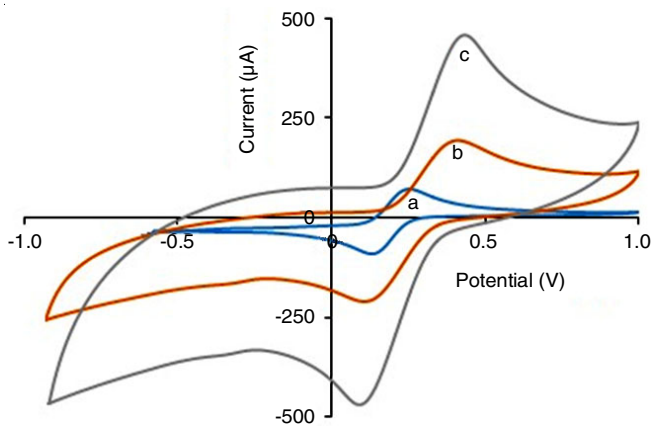

Fig. 5. Cyclic voltammogram of (a) GCE, (b) *p*-MWCNT-EVA nanocomposite film electrode, (c) *f*-MWCNT-EVA nanocomposite film electrode

Conclusion

In summary, we have developed a flexible, sheet-type conductive nanocomposite with MWCNT and EVA adhesive films. Surface functionalization of CNTs by carboxylic group affects the physical and electrochemical property of nanocomposite films. Chemical oxidation of CNTs creates carboxylic function at the *p*-MWCNT (powder) surfaces which in turn facilitates better electron transfer behaviour in *f*-MWCNT-EVA nanocomposite film as compared to *p*-MWCNT-EVA nanocomposite film. The chemical treatment also helps in their dispersion in ethanol, producing a uniform stable ink curable at room temperature for nanocomposite film development. The comparison of *p*-MWCNT-EVA and *f*-MWCNT-EVA nanocomposite films suggests that the surface functionalization increases the blending between carbon nanotube and EVA matrix as evident in SEM images. The results suggest that soft *f*-MWCNT-EVA nanocomposite films are a very promising conductive nanocomposites for the fabrication of flexible electrochemical platform which can be used for immobilization of biomolecules at the *f*-MWCNT-EVA nanocomposites film surface needed in biosensor development.

ACKNOWLEDGEMENTS

The authors acknowledge the research funding from Department of Biotechnology, India under Women Scientist Scheme to Rachana Sahney (research grants No. BT/Bio-CARe /05/640/2014-15) and Department of Atomic Energy, Government of India, Board of Research in Nuclear Sciences (Grant No. 37(2)/14/22/2017-BRNS). Thanks are also due to Mr. Swagat Sarangi, Technical Head, Swasan Chemicals Pvt. Ltd., Mumbai, India for providing the EVA polymer.

CONFLICT OF INTEREST

The authors declare that there is no conflict of interests regarding the publication of this article.

REFERENCES

1. S. Choi, H. Lee, R. Ghaffari, T. Hyeon and D.H. Kim, *Adv. Mater.*, **28**, 4203 (2016); https://doi.org/10.1002/adma.201504150.

2. H. Dai, E.W. Wong and C.M. Lieber, *Science*, **272**, 523 (1996); https://doi.org/10.1126/science.272.5261.523
3. C.K. Adu, G.U. Sumanasekera, B.K. Pradhan, H.E. Romero and P.C. Eklund, *Chem. Phys. Lett.*, **337**, 31 (2001); https://doi.org/10.1016/S0009-2614(01)00159-2
4. A. Cao, Z. Liu, S. Chu, M. Wu, Z. Ye, Z. Cai, Y. Chang, S. Wang, Q. Gong and Y. Liu, *Adv. Mater.*, **22**, 103 (2010); https://doi.org/10.1002/adma.200901920
5. N. Rouhi, D. Jain and P.J. Burke, *ACS Nano*, **5**, 8471 (2011); https://doi.org/10.1021/nn201828y
6. L. Hu, D.S. Hecht and G. Gruner, *Chem. Rev.*, **110**, 5790 (2010); https://doi.org/10.1021/cr9002962
7. J. Hirotani and Y. Ohno, *Top. Curr. Chem. (Cham)*, **377**, 3 (2019); https://doi.org/10.1007/s41061-018-0227-y
8. N. Gopal, A. Saxena and R. Sahney, *Fuller. Nanotub. Carbon Nanostruct.*, **29**, 643 (2021). https://doi.org/10.1080/1536383X.2021.1878153
9. M. Lamberti, P. Pedata, N. Sannolo, S. Porto, A. De Rosa and M. Caraglia, *Int. J. Immunopathol. Pharmacol.*, **28**, 4 (2015); https://doi.org/10.1177/0394632015572559
10. C.H. See and A.T. Harris, *Ind. Eng. Chem. Res.*, **46**, 997 (2007); https://doi.org/10.1021/ie060955b
11. A. Kumar, K. Sharma and A.R. Dixit, *J. Mater. Sci.*, **55**, 2682 (2020); https://doi.org/10.1007/s10853-019-04196-y
12. H. Beitollahi, F. Movahedifar, S. Tajik and S. Jahani, *Electroanalysis*, **31**, 1195 (2019); https://doi.org/10.1002/elan.201800370
13. W. Jayathilaka, A. Chinnappan and S. Ramakrishna, *J. Mater. Chem. C Mater. Opt. Electron. Devices*, **5**, 9209 (2017); https://doi.org/10.1039/C7TC02965A
14. P.M. Parthangal, R.E. Cavicchi and M.R. Zachariah, *Nanotechnology*, **18**, 185605 (2007); https://doi.org/10.1088/0957-4484/18/18/185605
15. B. Philip, J. Xie, A. Chandrasekhar, J. Abraham and V.K. Varadan, *Smart Mater. Struct.*, **13**, 295 (2004); https://doi.org/10.1088/0964-1726/13/2/007
16. M. Delmas, M. Pinault, S. Patel, D. Porterat, C. Reynaud and M. Mayne-L'Hermite, *Nanotechnology*, **23**, 105604 (2012); https://doi.org/10.1088/0957-4484/23/10/105604
17. S.Y. Chew, S.H. Ng, J. Wang, P. Novák, F. Krumeich, S.L. Chou, J. Chen and H.K. Liu, *Carbon*, **47**, 2976 (2009); https://doi.org/10.1016/j.carbon.2009.06.045
18. X. Sun, T. Chen, Z. Yang and H. Peng, *Acc. Chem. Res.*, **46**, 539 (2013); https://doi.org/10.1021/ar300221r
19. J. Mannayil, S. Methattel Raman, J. Sankaran, R. Raman and J. Madambi Kunjukutan Ezhuthachan, *J. Physica Status Solidi (a)*, **215**, 1701003 (2018); https://doi.org/10.1002/pssa.201701003
20. B. Ribeiro, E.C. Botelho, M.L. Costa and C.F. Bandeira, *Polímeros*, **27**, 247 (2017); https://doi.org/10.1590/0104-1428.03916
21. J.N. Coleman, U. Khan, W.J. Blau and Y.K. Gun'ko, *Carbon*, **44**, 1624 (2006); https://doi.org/10.1016/j.carbon.2006.02.038
22. M. David-Pur, L. Bareket-Keren, G. Beit-Yaakov, D. Raz-Prag and Y. Hanein, *Biomed. Microdevices*, **16**, 43 (2014); https://doi.org/10.1007/s10544-013-9804-6
23. S. Park, M. Vosguerichian and Z. Bao, *Nanoscale*, **5**, 1727 (2013); https://doi.org/10.1039/c3nr33560g
24. J. Ge, G. Cheng and L. Chen, *Nanoscale*, **3**, 3084 (2011); https://doi.org/10.1039/c1nr10424a
25. H. Dai, N. Feng, J. Li, J. Zhang and W. Li, *Sens. Actuators B Chem.*, **283**, 786 (2019); https://doi.org/10.1016/j.snb.2018.12.056
26. C. Min, X. Shen, Z. Shi, L. Chen and Z. Xu, *Polym. Plast. Technol. Eng.*, **49**, 1172 (2010); https://doi.org/10.1080/03602559.2010.496405
27. R. Andrews and M. Weisenberger, *Curr. Opin. Solid State Mater. Sci.*, **8**, 31 (2004); https://doi.org/10.1016/j.cossms.2003.10.006
28. J. Du, J. Bai and H. Cheng, *Express Polym. Lett.*, **1**, 253 (2007); https://doi.org/10.3144/expresspolymlett.2007.39
29. S. Xu, O. Rezvanian, K. Peters and M. Zikry, *Nanotechnology*, **24**, 155706 (2013); https://doi.org/10.1088/0957-4484/24/15/155706
30. M. Naseri, L. Fotouhi and A. Ehsani, *Chem. Rec.*, **18**, 599 (2018); https://doi.org/10.1002/tcr.201700101
31. S. Meer, A. Kausar and T. Iqbal, *Polym. Plast. Technol. Eng.*, **55**, 1416 (2016); https://doi.org/10.1080/03602559.2016.1163601
32. C. De Lannoy, D. Jassby, D. Davis and M. Wiesner, *J. Membr. Sci.*, **415-416**, 718 (2012); https://doi.org/10.1016/j.memsci.2012.05.061
33. U. Riaz and S. Ashraf, *Nanostructured Polymer Blends*, 509 (2014); https://doi.org/10.1016/B978-1-4557-3159-6.00015-8
34. J.-M. Park, G.-Y. Gu, Z.-J. Wang, D.-J. Kwon and K.L. DeVries, *Appl. Surf. Sci.*, **287**, 75 (2013); https://doi.org/10.1016/j.apsusc.2013.09.069
35. D.S. Hecht, L. Hu and G. Irvin, *Adv. Mater.*, **23**, 1482 (2011); https://doi.org/10.1002/adma.201003188
36. C. Niu, *MRS Bull.*, **36**, 766 (2011); https://doi.org/10.1557/mrs.2011.213
37. M. Sabet, H. Soleimani and S. Hosseini, *J. Vinyl Additive Technol.*, **24**, E177 (2018); https://doi.org/10.1002/vnl.21628
38. S. Azizi, C.M. Ouellet-Plamondon, P. Nguyen-Tri, M. Frechette and E. David, *Compos., Part B Eng.*, **177**, 107288 (2019); https://doi.org/10.1016/j.compositesb.2019.107288
39. Y. Li, Y. Lv, Z. Guo, L. Dong, J. Zheng, C. Chai, N. Chen, Y. Lu and C. Chen, *ACS Appl. Mater. Interfaces*, **10**, 15888 (2018); https://doi.org/10.1021/acsami.8b02857
40. A.F. Osman, A.M. Alakrach, H. Kalo, W.N.W. Azmi and F. Hashim, *RSC Advances*, **5**, 31485 (2015); https://doi.org/10.1039/C4RA15116J
41. N. Genina, J. Holländer, H. Jukarainen, E. Mäkilä, J. Salonen and N. Sandler, *Eur. J. Pharm. Sci.*, **90**, 53 (2016); https://doi.org/10.1016/j.ejps.2015.11.005
42. D. Lopes, M.J. Ferreira, R. Russo and J.M. Dias, *J. Clean. Prod.*, **92**, 230 (2015); https://doi.org/10.1016/j.jclepro.2014.12.063
43. A.M. Henderson, *IEEE Elec. Insul. Mag.*, **9**, 30 (1993); https://doi.org/10.1109/57.249923
44. K.A. Wepasnick, B.A. Smith, K.E. Schrote, H.K. Wilson, S.R. Diegelmann and D.H. Fairbrother, *Carbon*, **49**, 24 (2011); https://doi.org/10.1016/j.carbon.2010.08.034
45. V. Datsyuk, M. Kalyva, K. Papagelis, J. Parthenios, D. Tasis, A. Siokou, I. Kallitsis and C. Galiotis, *Carbon*, **46**, 833 (2008); https://doi.org/10.1016/j.carbon.2008.02.012
46. M. Deborah, A. Jawahar, T. Mathavan, M.K. Dhas and A.M.F. Benial, *Spectrochim. Acta A Mol. Biomol. Spectrosc.*, **139**, 138 (2015); https://doi.org/10.1016/j.saa.2014.12.041
47. W. Feng and P. Ji, *Biotechnol. Adv.*, **29**, 889 (2011); https://doi.org/10.1016/j.biotechadv.2011.07.007
48. J. Schönherr, J.R. Buchheim, P. Scholz and P. Adelhelm, *J. Carbon Res.*, **4**, 21 (2018); https://doi.org/10.3390/c4020021
49. P. Papakonstantinou, R. Kern, L. Robinson, H. Murphy, J. Irvine, E. McAdams, J. McLaughlin and T. McNally, *Fuller. Nanotub. Carbon Nanostruct.*, **13**, 91 (2005); https://doi.org/10.1081/FST-200050684
50. R.L. McCreery, *Chem. Rev.*, **108**, 2646 (2008); https://doi.org/10.1021/cr068076m
51. S. Sánchez, M. Pumera, E. Fàbregas, J. Bartrolí and M.J. Esplandiu, *Phys. Chem. Chem. Phys.*, **11**, 7721 (2009); https://doi.org/10.1039/b902710f
52. W. Cheung, P.L. Chiu, R.R. Parajuli, Y. Ma, S.R. Ali and H. He, *J. Mater. Chem.*, **19**, 6465 (2009); https://doi.org/10.1039/b823065j